NASA/TM–20260003401

Evaluating Energy Absorption Methods for Integrated Composite Seat Designs

Matlock M. Mennu, Jacob B. Putnam, Justin D. Littell, Nathaniel W. Gardner
Langley Research Center, Hampton, Virginia

May 2026

NASA STI Program Report Series

Since its founding, NASA has been dedicated to the advancement of aeronautics and space science. The NASA scientific and technical information (STI) program plays a key part in helping NASA maintain this important role.

The NASA STI program operates under the auspices of the Agency Chief Information Officer. It collects, organizes, provides for archiving, and disseminates NASA's STI. The NASA STI program provides access to the NTRS Registered and its public interface, the NASA Technical Reports Server, thus providing one of the largest collections of aeronautical and space science STI in the world. Results are published in both non-NASA channels and by NASA in the NASA STI Report Series, which includes the following report types:

- TECHNICAL PUBLICATION. Reports of completed research or a major significant phase of research that present the results of NASA Programs and include extensive data or theoretical analysis. Includes compilations of significant scientific and technical data and information deemed to be of continuing reference value. NASA counterpart of peer-reviewed formal professional papers but has less stringent limitations on manuscript length and extent of graphic presentations.

- TECHNICAL MEMORANDUM. Scientific and technical findings that are preliminary or of specialized interest, e.g., quick release reports, working papers, and bibliographies that contain minimal annotation. Does not contain extensive analysis.

- CONTRACTOR REPORT. Scientific and technical findings by NASA-sponsored contractors and grantees.

- CONFERENCE PUBLICATION. Collected papers from scientific and technical conferences, symposia, seminars, or other meetings sponsored or co-sponsored by NASA.

- SPECIAL PUBLICATION. Scientific, technical, or historical information from NASA programs, projects, and missions, often concerned with subjects having substantial public interest.

- TECHNICAL TRANSLATION. English-language translations of foreign scientific and technical material pertinent to NASA's mission.

Specialized services also include organizing and publishing research results, distributing specialized research announcements and feeds, providing information desk and personal search support, and enabling data exchange services.

For more information about the NASA STI program, see the following:

- Access the NASA STI program home page at http://www.sti.nasa.gov

- Help desk contact information:

https://www.sti.nasa.gov/sti-contact-form/
and select the "General" help request type.

NASA/TM–20260003401

Evaluating Energy Absorption Methods for Integrated Composite Seat Designs

Matlock M. Mennu, Jacob B. Putnam, Justin D. Littell, Nathaniel W. Gardner
Langley Research Center, Hampton, Virginia

National Aeronautics and
Space Administration

Langley Research Center
Hampton, Virginia 23681-2199

May 2026

Artificial Intelligence (AI) Usage Disclosure
This document was created with assistance from ChatGSFC for editing text. The content has been reviewed and edited by Matlock Mennu.

Available from:

NASA STI Program / Mail Stop 050
NASA Langley Research Center
Hampton, VA 23681-2199

Table of Contents

Table of Figures

Introduction

Composite materials have become ubiquitous in the aerospace industry due to their exceptionally light weight and high strength characteristics, as well as their unique ability to be engineered and tailored to meet specific loading conditions and performance requirements. These advanced materials offer superior strength-to-weight ratios compared to traditional metallic materials, making them particularly valuable in weight-critical aerospace applications where every pound saved translates to improved efficiency and performance. In currently operating fleets of commercial and military aircraft, composite materials have been successfully applied to critical structural components, including primary load-bearing elements such as the fuselage sections and flooring structures, which must withstand significant in-flight loads and provide passenger safety. Additionally, these materials have been specifically tailored and optimized for aerodynamic components such as wings and tail assemblies, where their ability to be molded into complex shapes while maintaining structural integrity is particularly advantageous. The application of composite materials extends beyond primary structural elements into the realm of internal cabin components, most notably in innovative seat designs where weight reduction and structural integration are paramount concerns. Modern composite seat structures can be designed to integrate multiple functions, including structural support, comfort features, and safety systems, all while maintaining the lightweight characteristics essential for aircraft performance.

According to established aviation safety standards and regulatory requirements, all seating systems must successfully pass stringent dynamic performance requirements during certification testing, with the critical evaluation metric being that lumbar load readings obtained from standardized Hybrid II or FAA Hybrid III Anthropomorphic Test Devices (ATDs) must remain below the mandatory 1,500-pound limit throughout the entire impact event duration [1,2]. This threshold represents a carefully established balance between occupant protection and structural feasibility, based on biomechanical research and accident investigation data that correlates lumbar loading with the risk of serious spinal injuries during aircraft crash scenarios. The Federal Aviation Administration (FAA) has established and published specific advisory circular (AC) documentation tailored for general aviation and rotorcraft vehicles that provides detailed methodologies and acceptable means for demonstrating compliance of seat designs using computer modeling analysis and simulation techniques [1]. This regulatory guidance represents a significant advancement in certification methodology, acknowledging that properly validated computational methods can provide equivalent or superior safety assurance compared to traditional physical testing approaches while reducing development costs and timelines. All newly developed seating systems intended for installation in rotorcraft, transport category airplanes, and small airplane categories must demonstrate full compliance with the rigorous performance standards established in Technical Standard Order TSO-C127b, which provides comprehensive performance criteria and testing requirements for aircraft seats based on the detailed technical specifications outlined in Society of Automotive Engineers (SAE) Aerospace Standard AS8049C [2, 3]. These standards establish minimum performance thresholds for structural integrity, occupant protection, flammability resistance, and emergency egress capabilities that all certified seat designs must meet or exceed. In addition to the mandatory performance standards, the aerospace industry has developed comprehensive recommended practices for implementing analytical methods in aircraft seat design and evaluation processes, as detailed in Aerospace Recommended Practice ARP5765 [4], which provides guidance on modeling techniques, validation procedures, and acceptable analysis methodologies. This document serves as a technical resource that helps engineers and certification authorities understand how to properly apply computational methods while maintaining the high safety standards required in aviation applications. Even though revolutionary new vehicle categories such as electric Vertical Take-Off and Landing aircraft (eVTOLs) and their associated seat designs may not directly fall under the existing regulatory categories established for traditional aircraft types, the comprehensive technical guidance and safety principles contained within these established documents will serve as guidelines and reference points for conducting thorough initial safety evaluations of such cutting-edge designs. This approach ensures that emerging technologies can benefit from decades of accumulated knowledge in safety while leading to the development of new, more appropriate regulatory frameworks tailored to these novel aircraft configurations.

In this current study, a composite airframe featuring an integrated composite seat structure was selected as the primary test article for a comprehensive research investigation. The integrated seat design differs from traditional airframes in that seat assemblies are structurally integrated with the fuselage rather than being mounted as separate components. This integrated design philosophy eliminates traditional mounting hardware, creating a more efficient load path distribution while reducing overall vehicle complexity, though it presents unique challenges for occupant protection analysis and certification compliance. Integrated composite seat designs can pose engineering and financial challenges during the testing and validation phases required for compliance certification (using previously established design requirements) primarily due to the complex structural interdependence created when the fuselage structure is permanently attached to and integrated with the designed seat assemblies. This integration means that traditional component testing methods may be insufficient, as the seat cannot be evaluated independently from the surrounding fuselage structure. Sophisticated testing approaches may be required to account for the combined structural behavior of the integrated system. Additionally, integrated composite seat designs raise unique engineering challenges in terms of applying conventional energy mitigation strategies that have proven successful in traditional seat mounting systems. Again, this is primarily due to the structural integration with the fuselage framework that eliminates the typical isolation between seat and airframe structure. This integration means that energy absorption mechanisms cannot be implemented as separate, modular components but must be carefully incorporated into the primary load-bearing structure without compromising the overall structural integrity or creating unacceptable weight penalties.

One economically viable method to explore this complex integrated design space is through the strategic utilization of test data to develop and validate computational models that can be used to iterate through seat designs focusing on maximizing occupant safety under various loading scenarios. These models serve as powerful tools that can significantly reduce the number of physical tests required while providing detailed insights into structural behavior, stress distributions, and failure modes that would be difficult or impossible to observe through physical testing alone. Therefore, the optimal approach is to consider energy absorption and occupant protection as integral aspects of the overall integrated design philosophy, rather than being added as secondary systems, requiring that safety mechanisms be incorporated directly into the original fuselage and seat structure design by seamlessly integrating them into the primary structural elements from the initial design phase. This approach requires close collaboration between structural engineers, safety specialists, and certification authorities to ensure that safety enhancements do not inadvertently compromise other critical performance requirements.

The research presented in this report will focus primarily on the methods of developing energy attenuation designs specific to integrated seating systems. It consists of a multi-scale test campaign followed by a detailed model development focused track. The test campaign consisted of both fuselage section only and full-scale vehicle impacts, which were designed to provide comprehensive data across multiple scales of structural response from localized seat performance to complete vehicle crash behavior. This multi-scale testing approach was essential for understanding how the integrated seat design performed both as an isolated component and as part of the complete structure during impact scenarios. Initial component-level tests consisting of isolated cockpit section assemblies extracted from the complete airframe were conducted using the 30-foot vertical drop tower facility located at NASA Langley Research Center (LaRC). These drop tests provided controlled impact conditions and localized instrumentation necessary to obtain performance data on the integrated seat structures when subjected to crash pulse loading with an occupant surrogate present. This controlled testing environment allowed researchers to focus specifically on seat performance without the complexity introduced by complete vehicle dynamics. A 50th percentile adult male FAA Hybrid III ATD was employed as the occupant surrogate in all conducted tests to ensure standardized biometric response measurements and maintain consistency. This specific ATD selection provides comparable injury assessment data that can be directly correlated with existing certification criteria and injury tolerance thresholds established through extensive automotive and aviation safety research. Additionally, two full-scale drop tests of fully instrumented complete composite airframes were conducted at the Landing and Impact Research facility (LandIR) located at NASA LaRC, which provides the capability for vehicle impact testing under controlled conditions to verify and validate the full structural response characteristics at the vehicle level during realistic crash scenarios [5]. These full-scale tests were essential for capturing the complex interactions between structural components and understanding how local seat performance impact overall vehicle crashworthiness behavior.

A commercial non-linear explicit finite element solver, LS-DYNA® [6], commonly used for solving complex dynamic impact problems involving large deformations, material nonlinearities, and contact interactions, has been selected as the primary computational tool for conducting comprehensive seat analysis in this research study. The initial test data set obtained from the component-level drop tower experiments was systematically utilized for calibrating and validating the material model parameters of the fuselage structure components, ensuring that the computational models could accurately represent the complex mechanical behavior. This behavior included the stiffness and failure of the composite structure along with energy absorption characteristics of the flight-representative composite structure under dynamic loading conditions. The calibration process involved iterative refinement of material properties, failure criteria, and contact definitions in LS-DYNA to achieve correlation between experimental measurements and analytical predictions within acceptable engineering tolerances. The experimental data collected from the first full-scale vehicle impact test was systematically employed to calibrate and refine the damage initiation and failure progression parameters of the developed composite material models, ensuring that the computational representations could accurately predict both the onset of structural damage and the subsequent failure propagation patterns observed in the physical tests. The model was then validated with a second full-scale test of a composite fuselage with an integrated seat by evaluating the model's performance in predicting the response of the structure as well as that of the occupant. This validation process was important for establishing confidence in the predictive capabilities of the material models across the full range of loading conditions and structural scales relevant to integrated seat design applications. These experimental investigations and subsequent model validation efforts led to the successful development of a composite material model that accurately captures the complex behavior of integrated composite structures under crash loading conditions, which could then be applied to generic fuselage design studies for systematic evaluation of different design modifications and safety enhancement mechanisms aimed at improving occupant protection in integrated seat designs.

After the test campaign, a generic composite fuselage model incorporating an integrated seat structure was developed and employed as a standardized platform for evaluating various design modifications and safety enhancements using the developed composite material model, with the primary research focus directed toward reducing occupant lumbar loads through the implementation and assessment of previously established and validated energy mitigation mechanisms. These mechanisms include specialized energy absorbing structures [7], advanced seat cushion systems [8], and optimized landing gear configurations [9], all of which have demonstrated effectiveness in traditional aircraft seat applications but require adaptation for integrated composite seat designs. The generic integrated fuselage design serves as a standardized baseline reference configuration that enables systematic and objective comparison of various design modifications and safety enhancement strategies for the integrated seat system, providing a consistent platform for evaluating the relative effectiveness of different approaches while controlling for variables unrelated to the specific modifications being investigated. This baseline approach is essential for developing reliable design guidelines and optimization strategies that can be applied to specific aircraft configurations while maintaining confidence in the comparative results. The detailed geometric modeling approach, comprehensive finite element model setup procedures, and systematic analysis methodologies employed in this research study are discussed and documented in this paper. This includes material model implementation details, boundary condition specifications, and loading condition definitions necessary for accurate simulation of integrated seat performance.

The main objective of the developed computational model is to provide a reliable evaluation of occupant loading conditions, with particular emphasis on the lumbar load experienced by seated occupants during various impact events and crash scenarios. Evaluating the resulting lumbar loads over a range of conditions enables a systematic optimization of the integrated seat design minimizing injury risk while maintaining structural integrity and certification compliance. This focus on lumbar loading points towards the critical importance of spinal protection in aircraft crash survival and the specific challenges posed by integrated seat designs in managing these loads effectively.

Model Calibration

A multi-phase approach incorporating experimental data from both sub-scale cockpit section and full-scale fuselage structural testing was utilized to establish material model parameters for the design study for integrated seats. The calibration process began with precise geometric reconstruction through high-resolution 3D scanning of the test specimens. This scanning data was subsequently processed to generate a detailed finite element mesh suitable for computational impact simulation analysis. The mesh resolution was optimized to capture critical structural features while maintaining computational efficiency for dynamic impact scenarios. Following mesh generation, the simulation framework was configured to replicate the initial conditions and boundary parameters observed during physical testing. Material model calibration was then carried out using key parameters including structural stiffness properties from previous models and adjusting laminate thickness values. These adjustments continued until the computational results achieved reasonable match with the experimentally measured composite behavior. Upon calibration at the component level, the updated material parameters were integrated into a full-scale structural model for validation. This final validation step was used to confirm that both the overall vehicle structural response and occupant dynamic response predicted by the simulation reasonably matched the corresponding experimental test data, thereby establishing confidence in the material model's predictive capability for design study using integrated composite seats.

The details of how this method was developed will now be described. Initially, the cockpit sections with integrated seats cut out from the full aircraft were 3D scanned to obtain the overall geometry of the test article. A hand-held 3D scanner from Creaform was used to capture the initial scan. VXelements, a software tool for importing scanned geometry, was used for cleaning up the scan, filling in the gaps and obtaining an initial finite element mesh. This mesh was imported into HyperWorks, a commercially available software for preprocessing and postprocessing explicit finite element model files, to create a detailed mesh for the cockpit section. Quadrilateral shell elements with an average size of 0.7 inches were used in addition to triangular shell elements accounting for less than 1% of the total number of elements. A total of two parts with 15,451 elements and 15,336 nodes were created.

The model development process relied on 3D scanning as primary means of reverse engineering, though this approach necessitated several critical assumptions regarding both the material system characteristics and structural layup configuration. First, due to the unknown nature of the actual composite material layup, the team assumed a quasi-isotropic layup configuration for the composite material system. This assumption provided a standardized baseline for material property calculations, though it potentially introduced variations from true structural behavior. Second, the modeling process assumed uniform thickness distribution across both the fuselage section and seat structure components, maintaining consistent dimensional properties throughout the scanned geometry.

These fundamental assumptions inherently limit the degree of model correlation that can be achieved through this reverse engineering process, primarily because the analysis relies on overall material properties rather than the actual discrete material characteristics present in the physical structure. In addition, limitations in 3D-scanning may further contribute to potential discrepancies between experimental testing results and computational simulation predictions. The integrated seat structure presents significant scanning challenges, as the surrounding fuselage geometry creates physical obstructions that prevent comprehensive three-dimensional scanning of the complete structural design. Lastly, the unknown composite layup sequence and any supplementary materials—such as core foam systems—can substantially alter both the bending stiffness characteristics and shear property responses of the overall structure. Consequently, the model calibration process requires several iterative refinement steps to achieve acceptable correlation with experimental data. Throughout the iterative modeling process, both the layer thickness parameters and material stiffness properties were adjusted to optimize correlation with drop test response data. This calibration method involved using the acceleration time-history curves measured at the seat base location as the benchmark for model calibration.

The test setup for calibration involved the use of the 30-foot drop tower at LARC. The cockpit section of the fuselage was mounted on the drop mass in the tower, and the system was released to impact at a velocity of 30 ft/s. A graduated paper honeycomb stack was located on the base plate to generate a 31g pulse resembling a Part 27 input pulse into the fuselage. Accelerometers were mounted on the base plate as well as in the cockpit section. A 50^{th} percentile male Hybrid III Male ATD was used for capturing the occupant response during this test. For the computational model, the fuselage structure and seat geometry were assigned *MAT_58 for a laminated composite fiber obtained from previously validated plain carbon weave composite models [10] developed at LaRC. A quasi-isotropic layup with a total thickness of 0.2 inches was used for the composite material model of the fuselage as well as the seat. The 50th percentile Hybrid-III ATD FEM model version 151214_BETA [11] was used in the simulation to represent the ATD employed in the drop tower test. Contacts were defined for the three-point restraint system securing the occupant into the seat using *AUTOMATIC_SURFACE_TO_SURFACE card for seatbelt to waist and torso, the fuselage and seat part set to the ATD part set as well as the full vehicle to the impact surface. In addition, the fuselage was constrained for the first 0.1 seconds of simulation to allow the ATD to settle into the seat and add pretension of the seatbelts. The model used spring elements to pretension the seatbelts to the ATD before switching them into rigid parts after 0.1 seconds. The impact plate was made using shell elements defined as a rigid part. The acceleration data collected from the baseplate of the drop tower test was used as the driving boundary condition of the impact plate. An accelerometer was placed at the base of the seat using *ELEMENT_SEATBELT_ACCELEROMETER at a similar location to that used in test configuration. The full simulation was run to 0.2 seconds. The simulation was run on a LINUX computer cluster using 8 processors and LS-DYNA version R13.1 double precision. The total time for the simulation to be completed was 12 hrs. Test and analysis results were filtered to standards defined in SAE J211 [12].

The model was calibrated by adjusting the thickness of the composite layup used to model the seat and the fuselage. Thickness of 0.2 inches provided sufficient compliance to represent the test results. To verify the model calibration, simulation predicted acceleration obtained from the ATD were compared to drop tower test results. Chest and pelvis acceleration as a function of time for the test and the simulation have been plotted in **Figure 1**. The chest acceleration showed an initial peak of 21.9 g followed by a secondary peak of 27.3 g for the test while the simulation showed peak accelerations of 26.3 g and 31.6 g respectively. The response of the simulation has similar phase to the testing with a slight difference in peak magnitudes. For the pelvis acceleration, the initial peak acceleration observed in the test data was 29.1 g compared to 26.3 g in the simulation showing a 9.6% difference. Based on these results, the material properties obtained were deemed acceptable to evaluate a full-scale vehicle test result to quantify the model's applicability in representing the structural material of a realistic eVTOL fuselage.

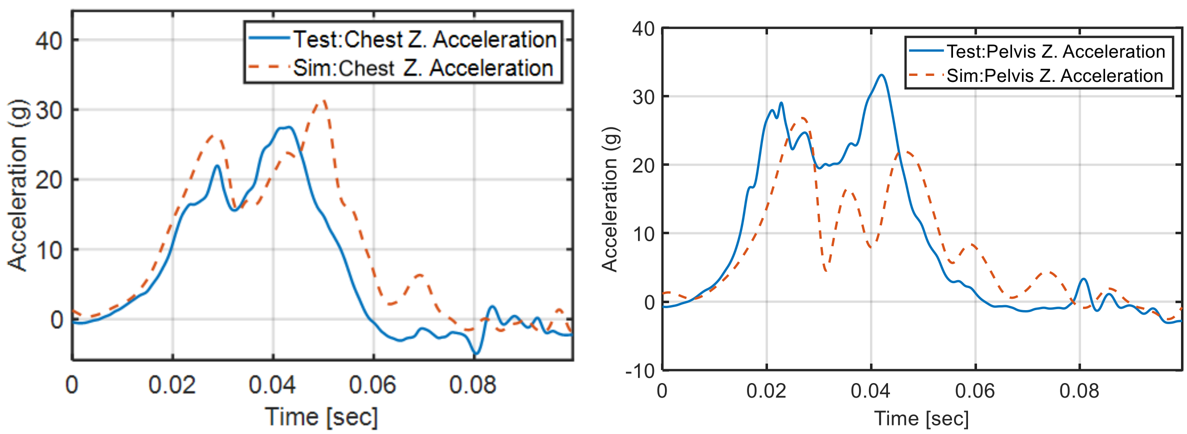

a. **b.**

Figure 1: a) Chest and b) Pelvis acceleration comparison between simulation and testing

Model Validation: Full Scale Test

In the first of two full-scale tests, the entire aircraft was present which included the tail section and landing gear. Before doing a detailed comparison, additional calibration was necessary for the landing gear component of the vehicle. Before conducting the initial full-scale test, accelerometers were placed along the length of the fuselage as well as across the wings. Accelerometers captured all three axes in the longitudinal (x-axis), lateral (y-axis) and vertical (z-axis) directions. An instrumented 50^{th} percentile male ATD was also used for the full-scale test for comparison with previous tests and models. The seat orientation in the fuselage was recumbent, allowing the occupant to sit in a laid-back position. A three-point restraining system was mounted on the vehicle and used to secure the ATD. A drop test was conducted from 14 feet based on emergency landing dynamic conditions and previous testing conducted at NASA LARC [13]. The test conditions were recorded using high speed cameras, instrumentation in the ATD and accelerometers mounted on the seat. The geometry of the full vehicle was obtained through a 3D scan similar to the fuselage section testing. A component of this aircraft scan, particularly the tail section, was merged with the previously generated model with the same mesh size. The landing gear was manually generated and included in this model. Frames from the high-speed test video were used to align the initial condition of the aircraft before impact. A 5° pitch down was included by rotating the impact plate and adjusting the acceleration vector for gravity accordingly. The stiffness and failure strain of the composite material for the landing gear was calibrated to account for the failure observed during testing. These values were adjusted to match the overall timing of the main impact events such as landing gear strike, nose impact and tail strike. The simulation was conducted with LS-DYNA version 13.1 double precision using 8 CPUs on a

Linux cluster. A three-point restraining system was used to secure the ATD model to the seat. Contacts were defined between the ATD, seat, fuselage, and the impact surface. The simulation ran for a total of 0.2 seconds with the first 0.1 seconds used for settling the ATD into the seat pan followed by 0.1 seconds for the impact event.

The comparative analysis results between experimentally measured acceleration data at the seat base location and corresponding simulation predictions are presented in **Figure 2**. The experimental test data reveals three distinct acceleration peaks that correspond to sequential impact events during the crash sequence. The first peak occurs at approximately 12 milliseconds and represents the initial landing gear ground strike event. The second peak occurs at 26 milliseconds, corresponding to the primary fuselage impact with the ground surface. Finally, the third peak appears at 77 milliseconds and correlates with the tail section slap-down event as the aircraft completes its impact sequence. The computational simulation results demonstrate excellent phase correlation with the experimental test signal, accurately capturing the timing and sequence of the three primary impact events. However, the simulation exhibits reduced correlation accuracy in terms of both the overall slope characteristics of the acceleration curves and the absolute magnitude values when compared to the experimental measurements. Despite these quantitative differences in slope and magnitude, the overall simulation acceleration curve shows that the dynamic response timing and impact sequence are well-represented in the computational model. These comparative results provide evidence that the developed composite material model serves as a reasonably representative approximation of the actual physical material system employed in the tested vehicle structure. The first full-scale test was utilized to capture the overall structural behavior of the full test article. Detailed comparison of occupant response was not performed for the initial test due to some discrepancies with data obtained from the ATD. While opportunities exist for further refinement of the material property parameters to improve magnitude and slope correlation, the current model demonstrates sufficient fidelity to capture the fundamental dynamic behavior and impact response characteristics of the integrated seat and fuselage system during crash events.

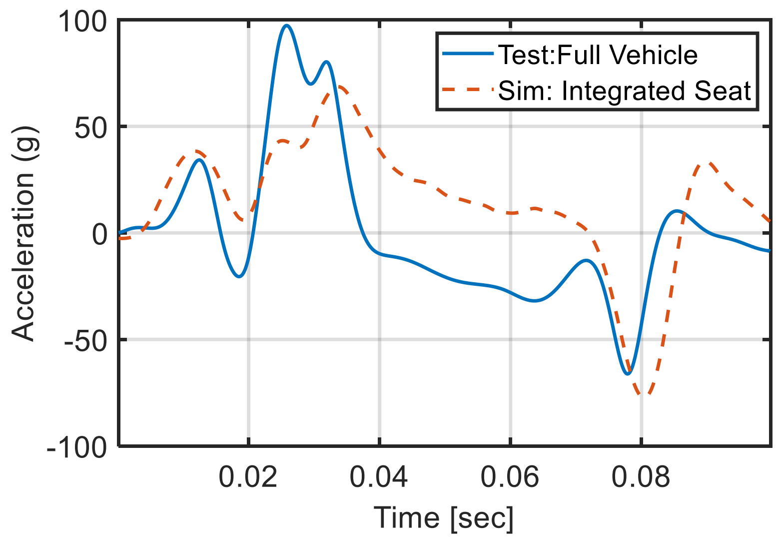

Figure 2: Seat Base Acceleration Comparison for Full Scale Test

A second full-scale test using a second composite airframe, identical to the one used in the first test, was conducted as a final step for model validation. In addition, cushions were added to the composite airframe to reduce the accelerations and loads into the ATD. A 1-inch honeycomb layer was placed on top of a 2-

inch polyester foam for the seat pan. The 2-inch polyester foam was also used in the seat back. The test was conducted outdoors at the NASA LandIR Facility. The vehicle was hoisted 14 feet to obtain a 30 ft/s impact velocity by using two straps mounted at the root of the wings and a third strap looped around the nose of the vehicle to position the airframe for a level impact.

For this validation test, a total of four high-speed cameras were positioned around the airframe and impact location. Two cameras utilized for high-speed three-dimensional Digital Image Correlation (3D-DIC) were positioned perpendicular to the port-side of the vehicle, viewing a speckled portion of the cockpit. A single high-speed camera used for viewing the entire airframe and marker tracking was positioned perpendicular to the starboard-side of the vehicle. Finally, a single high-speed camera was positioned in front of the airframe, perpendicular to the nose, and tilted slightly downwards capturing wingtip to wingtip. This camera was used primarily to observe the ATD motion in the seat, as well as to provide the ability to measure any roll of the vehicle prior to impact. The cameras were synchronized with respect to each other and shared a common, middle-trigger recording function. All cameras were synchronized with an IRIG timecode for direct comparison between camera data and DAS data utilizing a common timecode posttest. The cameras were set up to acquire images at 1000 Hz (1 kHz) with a continuous write-overwrite loop to the cameras buffer until the manual trigger event.

High-speed photogrammetry, more specifically full-field 3D-DIC and marker tracking, was implemented during the test. 3D-DIC was selected as the primary measurement technique to characterize the full-field displacement and strain of a portion of the cockpit on the port side of the test article. This non-contact optical technique was used to measure deformation on the surface by tracking the movement of the speckle pattern and subsequent pixel gray-scale variation during the test. Marker tracking was used to track the two-dimensional position and motion of bowtie markers that were manually placed in specific areas of interest to acquire impact conditions and subsequent motion of the vehicle. For this test, the impact conditions included vertical velocity, pitch and roll.

The results obtained from the testing are discussed below. The integrated composite fuselage was instrumented with accelerometers along the length of the fuselage. Vertical acceleration (z- acceleration) from triaxial accelerometers placed at the nose, base of the integrated composite seat, midsection where the landing gear is mounted, as well as on the tail are plotted in **Figure 3**. The high-speed video showed an vertical impact velocity of 28.4 ft/sec with 5.6 degree nose-down and 3.3 deg port-side down roll. Nose acceleration data shows a peak value of approximately 80 g which occurs 0.014 seconds after impact. The seat base accelerometer also measured a spike in acceleration at this time, but a higher value of 64 g occurred later at 0.025 seconds after impact. The landing gear/mid-section of the fuselage shows an initial ramp in acceleration up to 50 g at 0.021 seconds followed by a rapid unloading due to the contact of the bottom section of the fuselage to the impact floor. The tail acceleration peaks at a much later time of 0.075 seconds at 158 g due to tail strike.

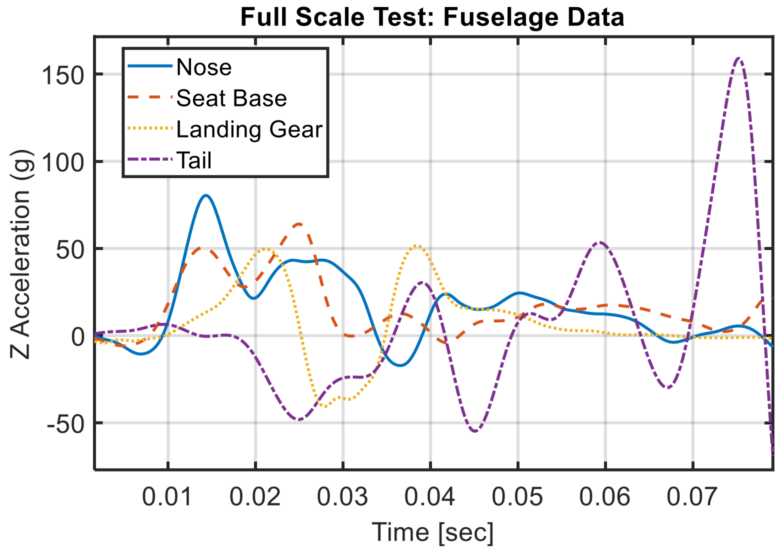

Figure 3: Acceleration measurement on the fuselage for full scale test

Accelerations were also measured on the wing tips. Vertical acceleration from both wings is shown in **Figure 4**. The oscillatory response of the wings is produced for both sections of the wing in the port and starboard sides. The peak acceleration measured was close to 100 g on the starboard side, which dampens out beginning approximately 0.1 s after the initial impact. The port side wing experiences similar behavior but produces a smaller peak value of 82 g. The overall impact response of the vehicle was as expected. The fuselage and the wings acceleration measurements confirmed the response observed through high-speed videos.

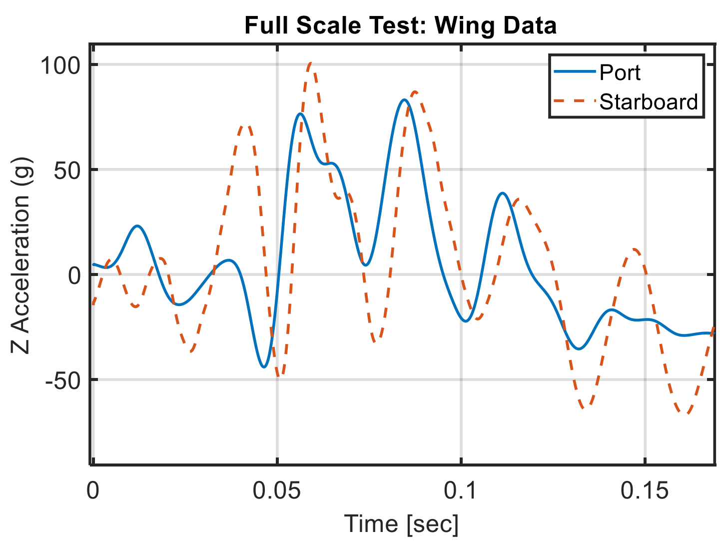

Figure 4: Acceleration measurement on each wing for full scale test

A section of the fuselage, just behind the cockpit, had a high-contrasting, random, black and white stochastic speckle pattern applied using a custom-made vinyl stencil pattern with a speckle size of approximately 0.25 inches. This area of interest had a reinforced layer of composite where the seat and landing gear were attached. Two high-speed VEO-640 cameras, affixed with 50 mm lenses, were focused on this section to obtain data from DIC. Even though cameras were positioned in a stereo configuration and calibrated to capture 3D displacements and strains, one camera was occluded by the wing deformation during impact. Therefore, 2D DIC was utilized to capture the change in strain behavior without necessarily determining the actual magnitude of deformation. The strain measurements captured before and after impact are shown in **Figure 5**. The purple color represents the minimum (negative) value, while the red color represents the maximum (positive) value. Prior to impact, low strain measurements were observed while in free fall due to rigid body motion (Figure 5a). After impact, the fuselage section shows a rapid onset of composite fracture. The initial crack forms at the bottom of the fuselage showing positive strain concentrated in the middle of the measurement area, as seen in Figure 5b. At maximum deflection during impact, the bowing of the fuselage is captured by a large positive strain in the mid-section and negative strains around the edges as seen in Figure 5c. This cracking phenomenon only occurred on the port side while no crack propagation was observed on the starboard side.

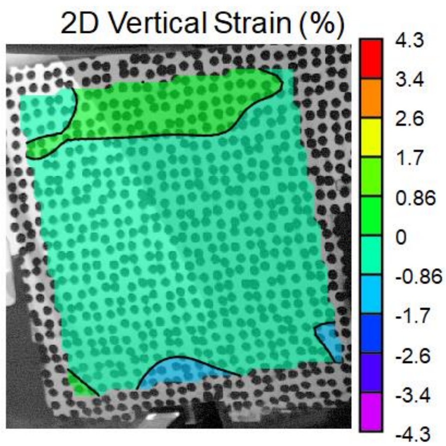

a.

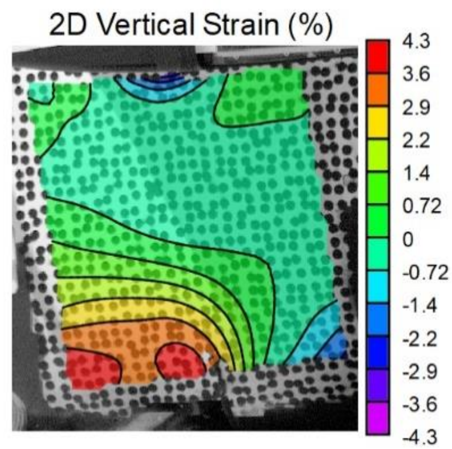

b.

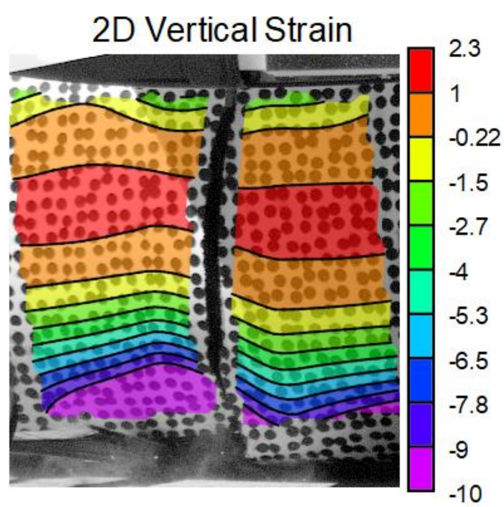

c.

Figure 5: a) 2D strain before impact, b) 2D strain during initial impact, and c) 2D strain during maximum deflection

A comparison between the head, chest and pelvis of the body in the vertical direction of the ATD during impact is shown in **Figure 6**. Peak acceleration values measured for the pelvis were 43.7 g followed by the head at 33.7 g and the chest at 29.4 g. The head experiences negative acceleration since the head is free to rebound after impact compared to the other parts of the body that were restrained by the seat belt.

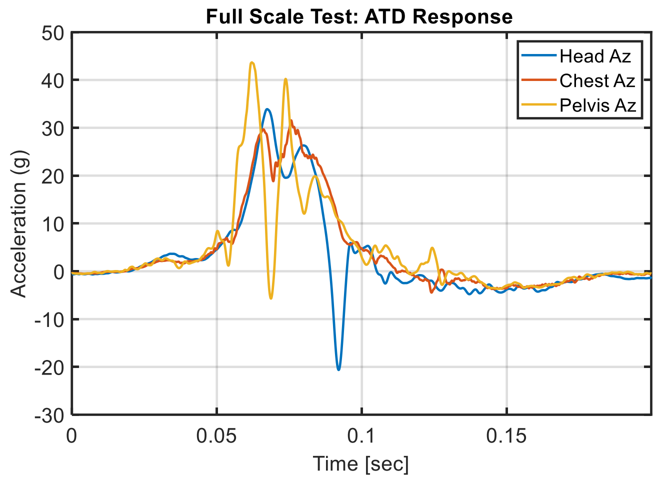

Figure 6: Head, chest and pelvis acceleration measurement in ATD for the full-scale test

Since the seat orientation is recumbent, a comparison between the longitudinal (x) and vertical (z) acceleration for each body section is presented below, in **Figure 7**. The head acceleration measured a higher peak of 60 g in the x direction. This phenomenon is due to the head striking the top of the seat and rebounding. The chest experienced similar magnitudes of acceleration in both the x and z direction with peak accelerations of 30 g and 22 g occurring, respectively. In addition, the pelvis response also showed a magnitude of 40 g in both directions.

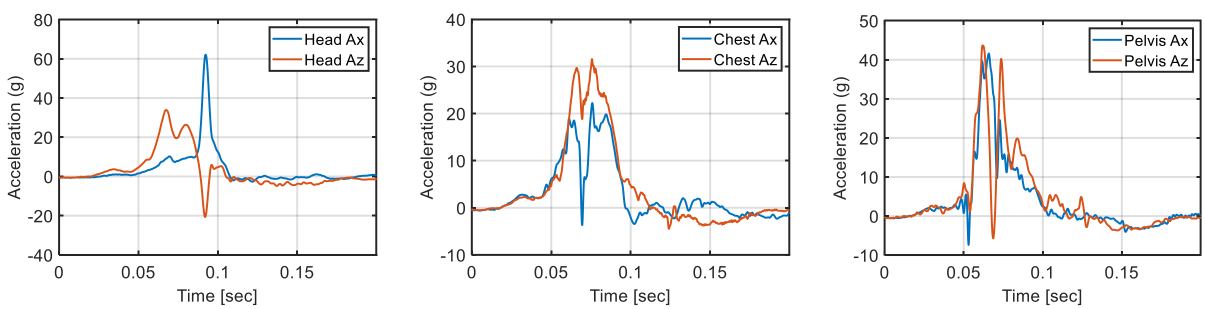

Figure 7: a) Head, b) Chest and c) Pelvis components in the longitudinal and lateral direction for recumbent seat used in the fuselage.

Loads measured in the lumbar region for both the vertical and longitudinal direction are presented in **Figure 8**. Compressive lumbar load, which is the measured lumbar load value in the z direction, is one factor used to determine injury to occupants. In this case, the maximum lumbar load in this direction was measured to be 1332 lb., which was below the FAA injury limit of 1500 lb. [14]. There was minimal load observed in the longitudinal direction with maximum load of 350 lb., which peaked at 0.075 sec after impact. This result showed that the lumbar load remains below the injury limit with the addition of cushion material for this impact condition.

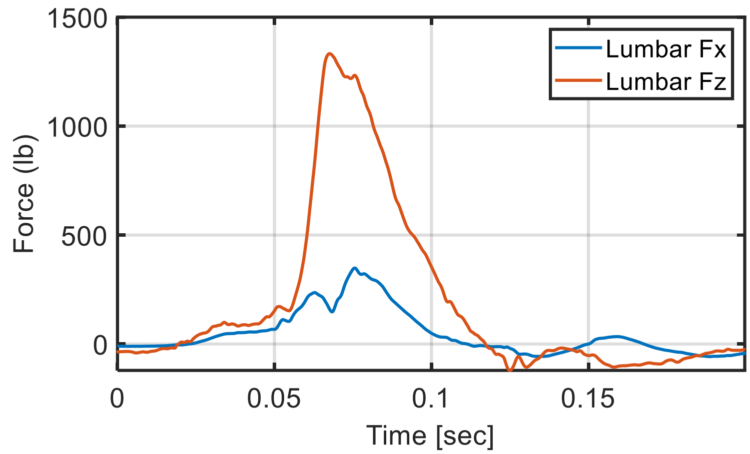

Figure 8: Lumbar load measured in the longitudinal and vertical direction in the ATD

Comparison of Airframe Response Between Simulation and Test

Once the analysis on the test was completed, an evaluation of the model was conducted by inputting the initial conditions from the test and comparing the results. The overall weight and pitch angle during impact was used to set up the model for running the impact simulation. In addition, the seat foam used in the recumbent seat was added to the model. The rest of the model remained the same with the previously described full-scale test simulation setup. The simulation ran for a total of 0.2 seconds with the last 0.1 second capturing the impact event.

The overall kinematic response of the entire vehicle was compared between the high-speed video and the simulation. The initial impact of the landing gear followed by the impact of the nose section and the tail strike showed close resemblance. A further quantitative comparison was performed between test and analysis, using the fuselage seat base acceleration response as in the previous test, as shown in **Figure 9**. The overall response of the vehicle was captured in the model with some notable differences. The test data exhibited a characteristic double-peak response with the first peak reaching approximately 50 g at 0.01 seconds and a dominant second peak of approximately 65 g at 0.025 seconds. Following these initial peaks, the test acceleration decayed rapidly to relatively low levels (0 to 20 g) by 0.04 seconds and remained at these low levels throughout the remainder of the event. In contrast, the simulation predicted a lower first peak of approximately 40 g at 0.015 seconds and second peak of approximately 35 g at 0.025 seconds. The simulation exhibited a maximum third peak reaching approximately 71 g at 0.035 seconds. The difference in peak magnitude between the test and simulation was less than 10%, however these peak magnitudes are offset in time by approximately 0.01 seconds.

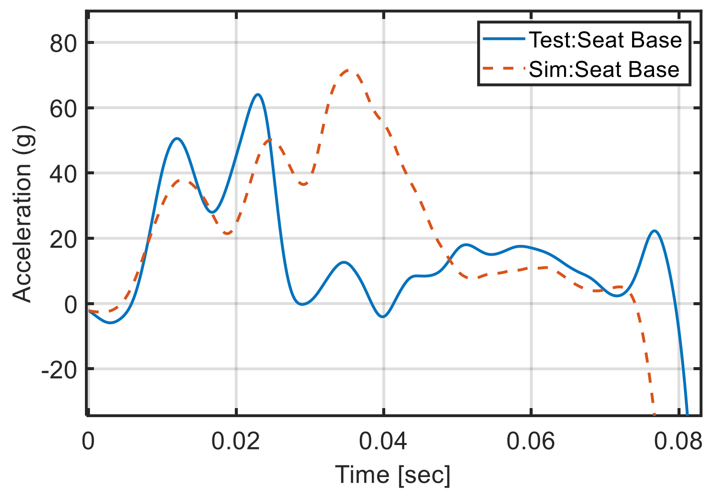

Figure 9: Seat Base Acceleration Comparison for Final Full-Scale Test

The presence of the third peak in the simulation at 0.04 seconds is likely due to elastic rebound of the fuselage structure following the initial impact loading. In the simulation, the seat base and underlying fuselage structure compress and deflect downward during the initial impact phase (0-0.025 seconds), absorbing kinetic energy elastically. As the structure rebounds between 0.025-0.04 seconds, the seat base separates from, or reduces contact with, the underlying structure, then re-impacts at approximately 0.04 seconds, creating the sharp 75 g acceleration spike. The simulation structure likely lacks adequate energy dissipation mechanisms such as structural damping, plastic deformation, and fracture that would prevent this elastic rebound. Additionally, the seat-to-floor interface may be modeled with insufficient compliance or damping, allowing rigid separation and re-contact rather than maintaining continuous contact through compliant connections.

From a validation and modeling perspective, this comparison highlights some limitations of the current simulation approach: the inability to predict and capture structural failure modes such as cracking and fracture. To capture the complete structural response, the simulation would require: (1) implementation of material failure models with appropriate failure criteria (e.g., maximum principal stress, plastic strain to failure, or fracture mechanics-based approaches); (2) detailed geometric and composite layup for accurate representation of composite stiffness in various areas; and (3) proper calibration of failure parameters based on material coupon testing. However, implementing these capabilities introduces significant complexity, computational cost, and uncertainty in predicting the exact location and timing of failure initiation. Fracture prediction in complex structures under dynamic loading remains challenging, even with advanced modeling techniques [15, 16].

Comparison of ATD Responses Between Simulation and Test

A comprehensive comparison of ATD responses between the simulation and the second full-scale test results is presented next, covering head, chest, and pelvis acceleration time histories. Overall, the simulation captured the key loading events and temporal sequence of the impact, though some differences in magnitude and timing were observed due to geometric and material modeling limitations.

The head acceleration response showed reasonable agreement in the initial loading phase, with both simulation and test exhibiting a similar rise time and initial peak magnitude of approximately 37 g and 34 g respectively, occurring around 0.03 seconds. This initial peak represents the head's upward acceleration as the ATD is subjected to the primary vertical impact event. However, differences emerged in the subsequent rebound phase. The simulation exhibited an immediate negative rebound with the head acceleration dropping to approximately -40 g around 0.04 seconds, indicating rapid whiplash dynamics as the neck extends and then rebounds. In contrast, the test data sustained a secondary positive peak of approximately 30 g at 0.04 seconds before transitioning to the negative rebound phase. This secondary peak in the test data suggests that the head contacted the seatback headrest during the initial upward motion, providing additional support and delaying the rebound. The subsequent negative rebound in the test reached approximately -20 g around 0.05 seconds, approximately 0.01 seconds after simulation's rebound timing.

The primary discrepancy between the simulation and test head response can be attributed to the seatback and headrest positioning. The exact position and orientation of the ATD relative to the seatback in the test configuration could not be precisely replicated in the simulation model. Specifically, the headrest position in the simulation appears to be further aft than in the actual test setup, resulting in delayed or absent head-headrest contact. This geometric difference fundamentally alters the head loading sequence: in the test, earlier headrest contact provides support and creates the observed secondary peak, while in the simulation, the head travels further without support before rebounding, leading to a different kinematic response. The timing offset of approximately 20-25 milliseconds between the simulation and test rebound events is consistent with this geometric mismatch. The head acceleration correlation demonstrates fair agreement given the known geometric limitations, with the simulation correctly predicting the general loading character (multi-peak response, rebound dynamics) but with timing offsets due to seatback positioning uncertainties. The head response is shown in **Figure 10**.

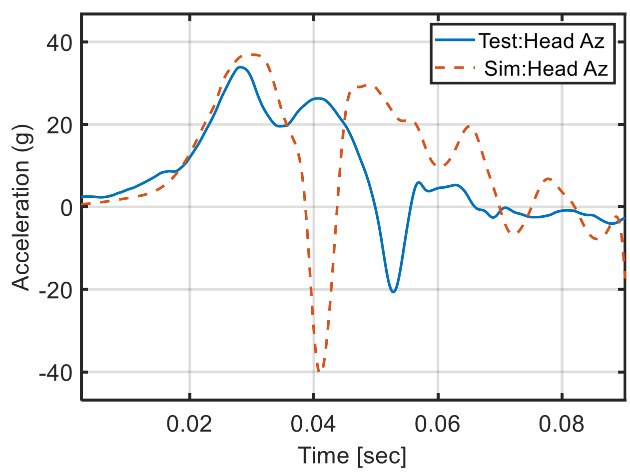

Figure 10: Head acceleration comparison between the test and simulation for the final full-scale test

The chest acceleration response, which is shown in **Figure 11**, demonstrated good overall correlation between simulation and test, with simulation over-predicting the initial peak acceleration. This multi-peak structure is physically representative of the complex loading sequence during vertical impact. The first peak, which occurred around 0.025 seconds, represents the initial upward acceleration of the torso as the impact load propagates from the pelvis through the spine to the chest. The second peak observed around 0.035 seconds corresponds to the maximum chest compression and/or secondary loading as the torso impacts and compresses against the seatback.

Both the simulation and test data showed a similar trend, validating that the simulation captured the fundamental loading physics. However, the simulation consistently over-predicts the chest acceleration magnitudes throughout the primary loading phase. The test results exhibited peak values averaging approximately 30 g, with the highest peak reaching 32 g around 0.03 seconds. In contrast, the simulation predicted peak accelerations of approximately 45 g, with the maximum occurring around 0.025 seconds. This represents an over-prediction of approximately 28% in peak magnitude. The timing of the peaks was well-aligned between simulation and test, with both showing the first peak at 0.025 seconds and the second peak around 0.04 seconds, indicating correct temporal phasing of the loading events.

The magnitude over-prediction in the chest response is attributed primarily to insufficient compliance modeling in the seatback structure. While the seat cushion foam layer (added between the seat base and ATD pelvis) successfully improved the pelvis correlation, the seatback likely contains additional padding or structural compliance that was not fully captured in the simulation model. The seatback in the simulation may be too stiff and lacks the ability to precisely predict failure, leading to higher transmitted loads to the chest. In predicting the shape and phasing of chest response, these results demonstrate the model is capturing the general physics of the loading transferred into the occupant though refinement through seatback compliance modeling would improve accuracy for injury prediction applications.

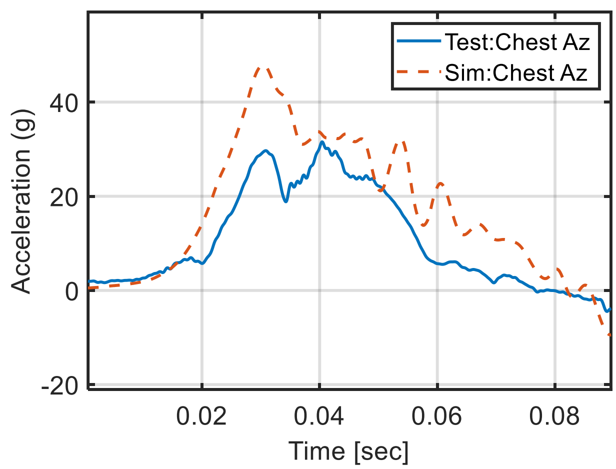

Figure 11: Chest acceleration comparison between the test and simulation for the final full-scale test

The pelvis acceleration response, which is shown in **Figure 12**, exhibited excellent correlation between simulation and test, representing the most successful validation result among all body regions. Both simulation and test displayed a characteristic double-peak loading response, with the initial peak occurring at approximately 0.035 seconds and a secondary peak at approximately 0.04 seconds. The test data showed peak magnitudes of approximately 43 g and 40 g for the first and second peaks, respectively. The simulation predicted peak values of approximately 43 g and 45 g, resulting in almost perfect match for the first peak, but overprediction of the second peak by approximately 13%.

The double-peak response observed in both simulation and test is physically representative of the pelvis impact sequence with a foam seat cushion. The first peak, which occurred at approximately 0.035 seconds, corresponds to the initial contact and compression of the seat foam as the ATD pelvis impacts the seat surface. The brief valley between peaks represents the progressive crushing of the foam cells as they compress under load. The second peak, which occurred at approximately 0.04 seconds) occurs as the foam approaches densification (cell walls contact each other) or as the underlying seat structure begins to engage, creating a stiffer load path. This progression—initial contact, foam compression, densification/structure engagement—is classic crushable foam behavior and indicates that the simulation correctly captured the seat cushion material response.

The pelvis response is critical in vertical impact scenarios as it represents the primary load path from the seat into the occupant. Achieving excellent pelvis correlation provides confidence that the fundamental impact mechanics—contact dynamics, energy transfer, and load distribution—are being captured by the model. This serves as the foundation for the entire kinematic chain, as loads propagate from the pelvis through the spine to the torso and head. The pelvis correlation quality (within 11% error, correct timing, correct character) demonstrates adequate correlation with the test data to provide confidence in the model's ability to predict pelvis acceleration in terms of shape, phase, and magnitude. [17]

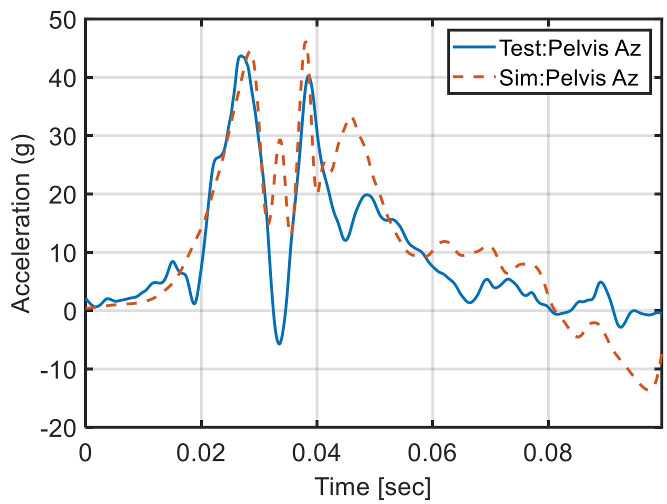

Figure 12: Pelvis acceleration comparison between the test and simulation for the final full-scale test

The lumbar force response demonstrated excellent overall correlation between simulation and test, with both exhibiting similar temporal phasing and characteristic loading patterns representative of vertical impact through the pelvis-spine load path. The test data showed a peak lumbar force of approximately 1330 lb. occurring around 0.035 seconds, while the simulation predicted a higher peak force of approximately 1460 lb. at 0.045 seconds as shown in **Figure 13**. This represents an over-prediction of approximately 9% in peak magnitude. Both curves exhibited a rapid rise from baseline starting around 0.02 seconds, reaching their respective peaks between 0.035-0.04 seconds, followed by a gradual decay back to near-zero levels at 0.08-0.09 seconds after impact. The general shape and duration of the loading pulse matched well between simulation and test, indicating that the fundamental load transfer mechanics through the lower spine were correctly captured.

The multi-peak response observed in the simulation (with peaks around 0.04 seconds and 0.045 seconds) corresponds to the double-peak characteristic observed in the pelvis acceleration response, confirming the direct mechanical coupling between pelvis motion and lumbar loading. As the pelvis experiences its initial impact and compression against the seat cushion (first pelvis peak), the lumbar spine is loaded in compression as it transmits forces from the pelvis to the chest. The secondary peak in lumbar force reflects the continued loading as the seat foam densifies or the seat structure engages, consistent with the second pelvis acceleration peak. The test data showed a smoother peak structure with less pronounced secondary oscillations compared to the simulation, suggesting that the actual ATD spine may have more internal damping or compliance that distributes the load over a slightly longer duration.

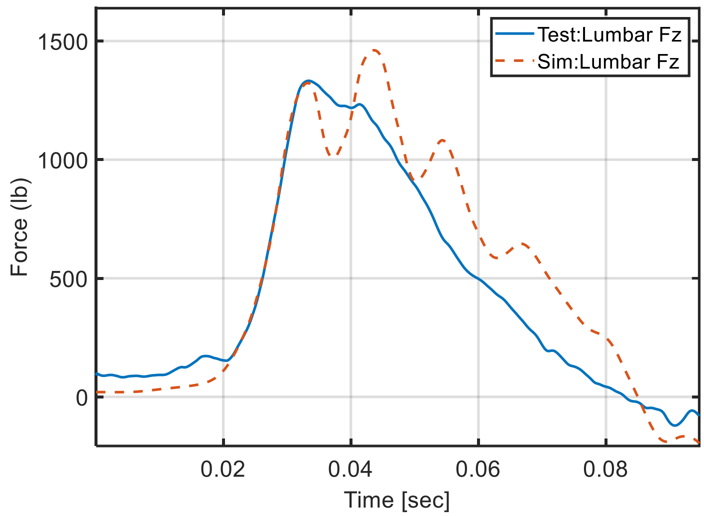

Figure 13: Lumbar spine compression comparison between test and simulation

From an injury assessment perspective, the lumbar force correlation has important implications for occupant safety evaluation. Lumbar spine compression is a critical injury mechanism in vertical impact scenarios, with injury thresholds typically defined at 1500 lb. for FAA seat certification of a 50^{th} male ATD [18]. The test showed a peak lumbar force of 1400 lb., which is below injury threshold, while the simulation predicted 1430 lb., which was still below threshold values for seat certification. The 9% over-prediction means the simulation is conservative (predicting higher injury risk than occurred), which is generally preferable to under-prediction from a safety standpoint. The excellent correlation shown in this model helps validate the use of this model specifically for comparing lumbar loads between various designs.

This lumbar force validation result, when combined with the pelvis acceleration correlation achieved earlier, provides strong confidence in the model's ability to predict lower-body injury metrics and support design optimization efforts aimed at minimizing lumbar compression during vertical impact crash events. The pelvis and lumbar spine represent the primary load path in vertical drop scenarios—where impact energy is absorbed by the seat cushion, enters through the pelvis, and is transmitted through the lumbar spine to the upper body—and achieves good correlation on both the pelvis and lumbar force validates that this fundamental load path is correctly modeled. This gives credibility to using the model for parametric studies to evaluate design changes such as varying seat cushion thickness, density, or material type; modifying seat structure stiffness or geometry; adjusting ATD positioning or restraint configurations; or optimizing energy absorption characteristics to minimize both peak accelerations and peak lumbar loads simultaneously.

Composite Fuselage Design

Geometry from a single passenger quadrotor vehicle concept developed by researchers at NASA Ames Research Center [19] was used to develop a concept fuselage model with integrated seats shown in **Figure 14**. A generic seat geometry was integrated into the fuselage structure, using HyperMesh to extrude the edges of the seat in the direction of the fuselage. The seat geometry consists of a generic seat pan and back rest with a front leg angled towards the aft mounted on the fuselage. Mesh was generated for this structure by insuring coincident nodes between the fuselage and the seat edges. The fuselage with the integrated seat used 22086 elements and 21959 nodes meshed into two parts. The main element type was quadrilateral shell elements with an average size of 0.95 inches, while additional triangular elements accounted for 0.1%

of the total count. The quasi-isotropic composite material model, validated in its definition of material system used in a realistic seat integrated composite fuselage, was used to define the material for the integrated seat structure. In addition, a windscreen was modeled using elastic material properties for polycarbonate plastic. The baseline model used a rigid fuselage definition to represent a bounding case in which the aircraft fuselage did not aid the integrated seat in energy absorption through its structure. The ATD model with the three-point restraining system, developed to analyze the proprietary vehicle model, was adapted to this vehicle configuration. The previously developed contact definitions were updated accordingly to include these parts and update the contact between the new integrated fuselage and the rigid impact surface.

Figure 14: Single Occupant Integrated Composite Seat Design

The simulation was conducted for a total of 0.2 seconds. The fuselage structure was restricted from motion by using *BOUNDARY_PRESCRIBED_MOTION for the first 0.1 seconds to allow for the ATD to settle into the seat. The initial velocity of 30 ft/s was defined to begin after this preload step. Measurements obtained from the ATD model were used for comparison between various fuselage models. The primary data of interest is the pelvis acceleration and lumbar load in the vertical direction for this drop test simulation. The results from the rigid fuselage structure are presented in **Figure 15**. The maximum pelvis acceleration measured was 95.9 g while the lumbar load peaked at 2429 lb., which is much higher than the occupant injury threshold of 1500 lb. This baseline design shows the behavior of the seat when attached to the rigid fuselage. Since seats cannot act independently to absorb impact energy, design considerations for integrated seats must account for the crash behavior of fuselage structure along with the seat design.

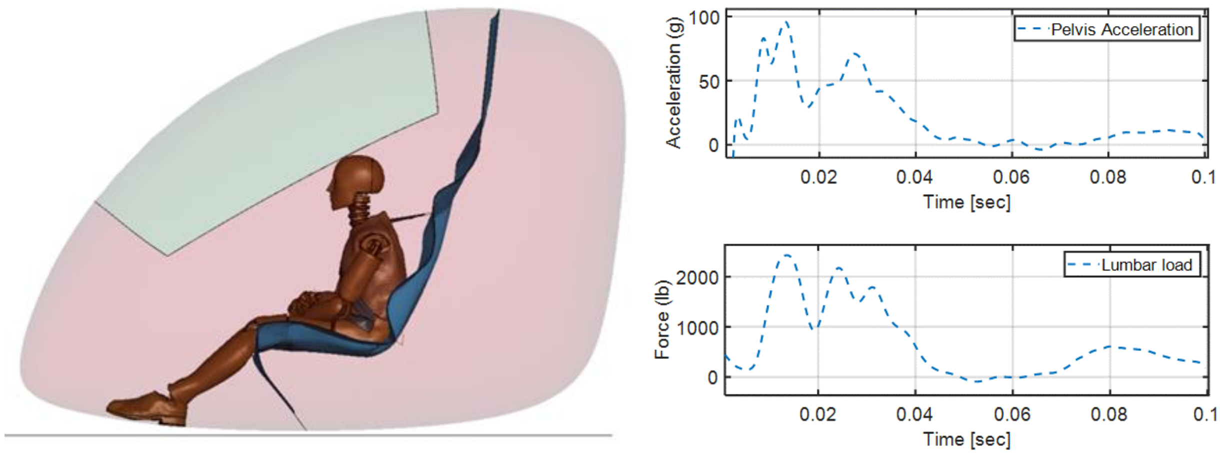

Figure 15: Simulation Result After Impact with Plot of Pelvis Acceleration and Lumbar Load

Energy Absorption Methods

Conventional methods such as seat stroking mechanism cannot be implemented easily for integrated seat designs. One option is to design the stiffness and geometry of the seat and fuselage structure to reduce the impact loads to the occupant. In addition, foam layers can provide an added layer of energy dissipation between the seat and the occupant. Another means of energy absorption includes separation of the seat from the fuselage during impact events. This presents a unique design challenge in ensuring structural integrity during normal operations, while allowing the seat to act independently during impact events. This can be further complicated by the increased complexity in manufacturing that would detract the intent of the integrated seat designs in the first place. These various techniques considered are presented in the order that they were evaluated.

The first model evaluated the effect of a compliant fuselage structure with the material properties obtained from the calibration and validation process discussed above. The results from the simulation showing a slight deformation of the fuselage and seat leg in addition to the pelvis and lumbar response are shown in **Figure 16**. Even though the deformation is limited, the use of composite material as the compliant structure for both the seat and fuselage deformed to reduce the peak pelvis acceleration from 100 g in the rigid structure to down to 50 g, approximately 50% reduction. In addition, the lumbar load reduced from 2300 lb. to closer to 1500 lb. (approximately 35% reduction) showing the composite fuselage is providing some means of energy absorption through deformation.

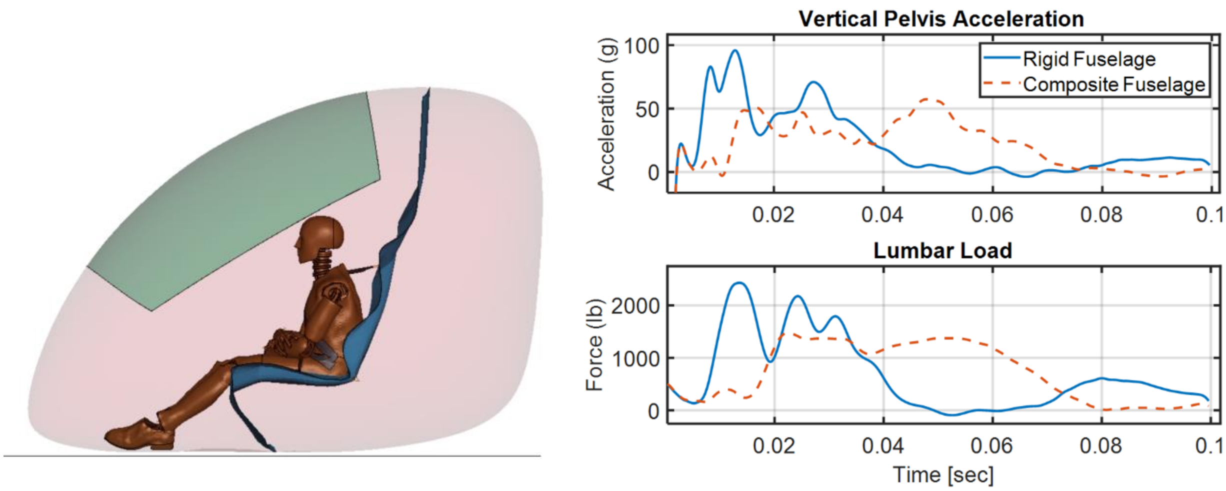

Figure 16: Composite Fuselage After Impact with Plot of Pelvis Acceleration and Lumbar Load Compared to Rigid Fuselage

The second iteration of the design looked to compare the initial composite fuselage design followed by adding polyurethane and polyethylene foams. A single layer of polyurethane foam with a thickness of 0.67 inches was included on the seat back rest and bottom. Another layer of polyethylene foam with a thickness of 0.2 inches was added to the bottom of the seat. The third iteration of the design updated the seat leg geometry. Previous studies have looked at using corrugated composite crush tubes to reduce occupant loading [20]. This design concept was incorporated in this study by modifying the seat base geometry to incorporate a corrugated structure under the seat as seen in **Figure 17**. The seat geometry was adjusted in HyperWorks. The seat and the fuselage were remeshed to ensure coincident nodes between the seat and the fuselage.

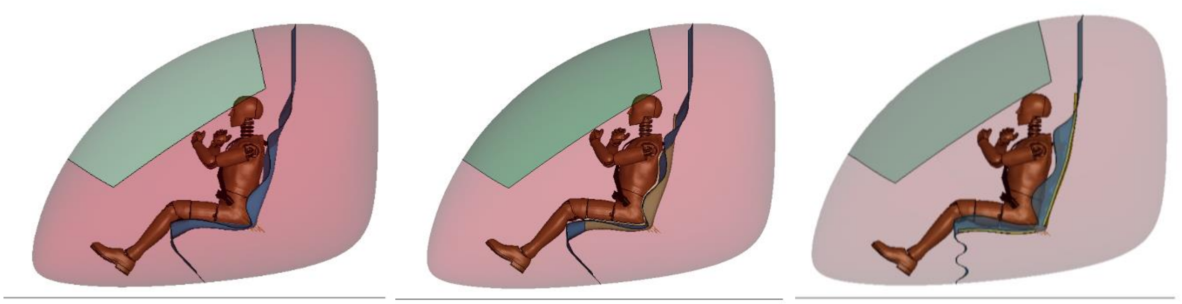

a. Initial Composite Fuselage design **b. Seat with foam** **c. Corrugated leg with foam**

Figure 17: First set of designs for an integrated composite seat fuselage

Simulations were run for the three design options (i.e. composite airframe, seat with foam, corrugated leg with foam) and the results for the pelvis acceleration and lumbar load were compared between these designs in **Figure 18**. The composite airframe design showed a maximum acceleration of 57 g, seat with foam had maximum acceleration at 53 g and the corrugated leg design with foam had a maximum acceleration of 55 g. These peak accelerations were approximately at 50 milliseconds after impact and dominated mainly by the deformation of the fuselage contacting the bottom aft section of the seat. When looking at the acceleration curve during the initial phase of impact, for the first 40 milliseconds, the acceleration of the corrugated seat is the lowest at 43 g while the initial design and seat with foam had 50 g. The corrugated design provided better initial response but wasn't sustained for the entire impact.

A similar comparison was made to the lumbar loads obtained from the simulation. The initial design showed a maximum force of 1469 lb. The seat with the foam layers had a maximum acceleration of 1415 lb. while the corrugated leg with foam showed a maximum load of 1519 lb. but occurs later at approximately 0.035 seconds. The addition of the foam layer provides a slight reduction in the loads transferred to the occupant. The corrugated leg design reduces the initial peak but gradually rises through the progression of the impact.

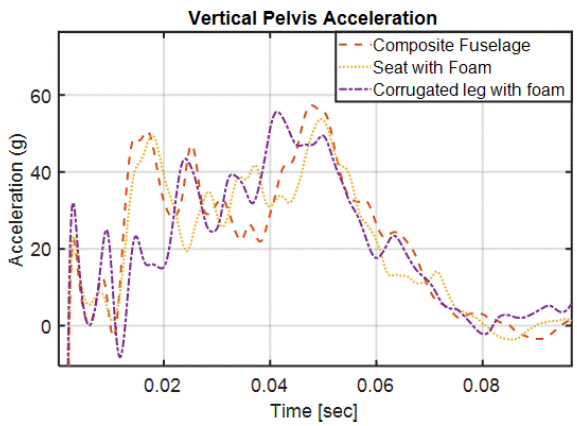

a.

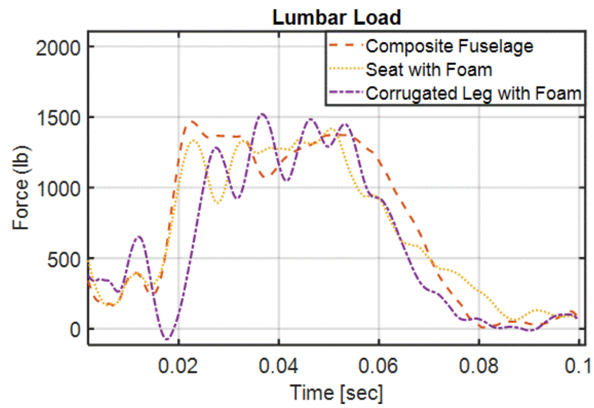

b.

Figure 18: a) Vertical pelvis acceleration comparison and b) Lumbar load comparison between various designs

The corrugated design showed some promising results during the initial phase of the impact but was not sustained throughout the impact event. Additional design iterations were evaluated to understand the utility of the corrugated seat design. The first study looked at an integrated fuselage seat mounted on the sides and top region without any composite structure under the seat. This structure relies on the deformation of the fuselage structure to absorb the impact energy. The second structure used a corrugated seat leg for the front section. The third structure added linear composite section for the aft leg to stabilize the seat during impact and reduce the induced neck rotation. All the models shown in **Figure 19** were updated in HyperMesh, and the simulation was conducted with LS-DYNA version 13.1 double precision using 8 CPUs on a Linux cluster. The model setup, configuration and contact definitions remained the same for all subsequent simulations.

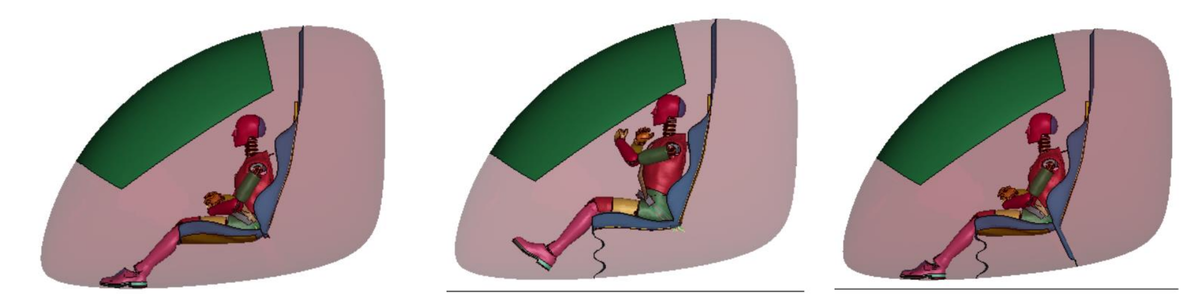

a. No legs **b. Single corrugated leg** **c. Corrugated leg with aft support**

Figure 19: Design iterations for an integrated composite seat fuselage

The pelvis acceleration results from the three designs are shown in **Figure 20**. The maximum deceleration measured in the fuselage with no seat legs had a magnitude of 166 g, followed by the corrugated seat with aft support at 56 g and the single corrugated seat at 55 g. The lumbar load was also compared between the three designs. The fuselage structure with no legs resulted in a lumbar load of 2800 lb. The corrugated seat with aft support produced a lumbar load of 1961 lb. and the single corrugated seat leg produced a lumbar load of 1519 lb. The single corrugated seat leg yielded the best results in terms of pelvis acceleration and lumbar load.

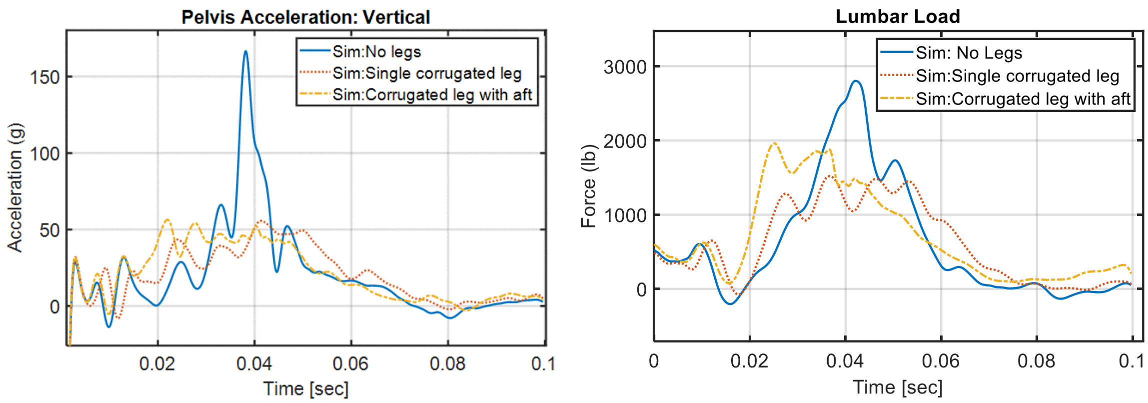

a. **b.**

Figure 20: a) Pelvis acceleration results and b) Lumbar load for various design iterations for the corrugated seat leg

This study was followed by adjusting the thickness of the corrugated seat leg with aft support to minimize this movement while aiming to achieve a survivable lumbar load of 1500 lb. In the first attempt, the leg thickness was increased by 50% compared to the baseline, followed by another study that decreased the leg thickness by 50%. There was a non-linear relationship between the thickness of the corrugated seat and ATD response as seen in **Figure 21**. When the leg thickness increased, the initial acceleration peak increased from 56 g to 90 g while decreasing the leg thickness resulted in a peak acceleration of 89 g. When the leg thickness decreased, peak acceleration occurred 15 ms. later compared to the other two cases (i.e. initial and 50% leg thickness increase) which correspond to the seat pan contacting the deformed fuselage underneath. Lumbar load results follow a similar trend, as increasing the leg thickness produced a load of 2858 lb. while decreasing the leg thickness produced a load of 2625 lb.

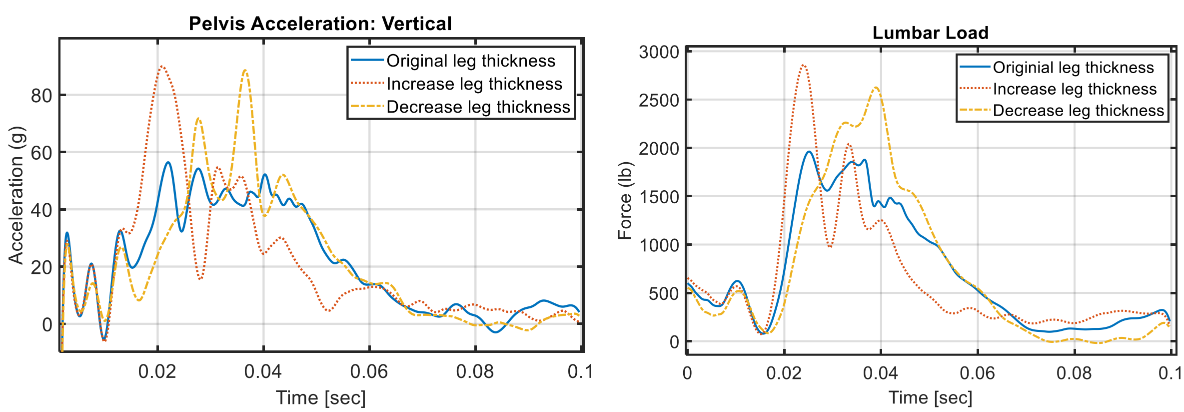

a. **b.**

Figure 21: a) Pelvis acceleration results and b) Lumbar load for varying corrugated seat leg thickness

Seat Separation Designs

For the final aspect of this composite airframe design investigation, the corrugated seat design was augmented with a frangible seat. This seat features a thin composite edge along the junction between the fuselage and the seat that can be used for energy mitigation during impact. The goal behind this design considers using similar manufacturing method as a conventional integrated seat design but reduce the ply at the edges of the seat so that energy can be absorbed through the failure of this composite layer around the edges of the seat. A subset of the seat geometry elements was selected and assigned to a different part named frangible seat. The top section of the seat was disconnected from the fuselage to allow for the seat to separate. This part was assigned a different composite material property using *MAT_COMPOSITE_FABRIC to account for this design. The plies used for this was $[0/90]_3$ with a total thickness of 0.048 inches. The cross-section model of this design is presented in **Figure 22**.

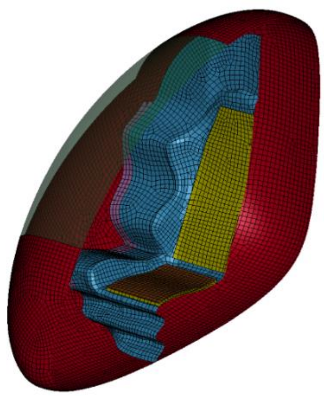

Figure 22: Cross-section View of Corrugated Frangible Seat

The previously evaluated impact conditions were simulated with this design. The updated seat design with the corrugated seats changed the exact depth of the seat pan, resulting in the translation of the ATD model to account for this change to remove any penetrations with the seat and foam layers. The three-point restraining system was also adjusted accordingly. The simulation was conducted for 0.2 seconds with the first 0.1 seconds used for settling the ATD into the seat. The acceleration results have been presented in **Figure 23**. The frangible joint design shows a maximum vertical pelvis acceleration of 50 g compared to the 55.5 g of the corrugated seat design and 57.3 g of the composite fuselage design. The lumbar load was also reduced to 1411 lb. compared to 1519 lb. of the corrugated seat and 1469 lb. of the composite fuselage design. This showed an overall reduction of peaks from the composite fuselage design by 7% and achieved loads below the injury threshold. The peak acceleration was reduced by 12% compared to the composite fuselage design.

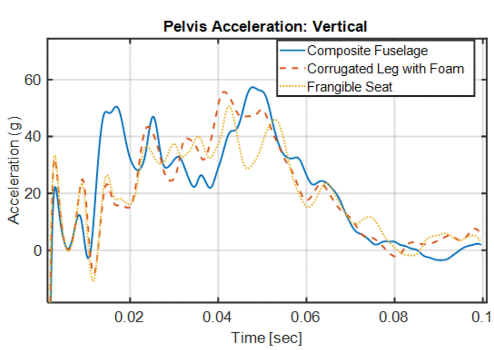

a.

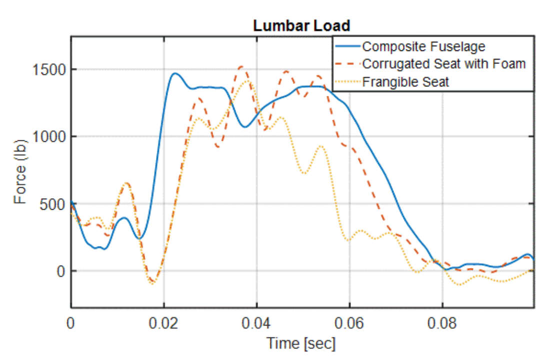

b.

Figure 23: a) Pelvis acceleration results and b) Lumbar load comparison for the frangible seat design

Discussion

Typical designs for fuselage structures and crashworthy seat designs require the separate development of seats, subfloor and fuselage to account for impact loads during emergency landing conditions. When integrated seats are used as part of the vehicle design, a systematic approach is necessary for adopting the design to ensure occupant safety. A single occupant composite fuselage design with integrated seat was developed to understand energy absorption techniques for this type of seat design. This generic fuselage design with integrated seat was used to evaluate components under the seat in conjunction with the fuselage that can be used to mitigate the impact loads into the occupant. The main driving force for large loads into the occupant is the stiffness of the fuselage since the seat structure cannot deform independently for such designs. Therefore, consideration must be taken to optimize the fuselage structure to ensure that it provides sufficient stiffness for the overall performance of the aircraft while also ensuring that there is compliance necessary to provide occupant protection during an off-nominal landing condition.

This research effort also successfully demonstrated the suitability of reverse engineering tools such as the integration of three-dimensional scanning technology, experimental testing for model calibration, full scale testing for model validation, and iterative computational modeling techniques for vehicle applications. The results shown have supplemented previous NASA research in showing that these methods can generally capture the fundamental dynamic response characteristics of composite airframe structures, despite the inherent challenges associated with unknown layup configurations and material system specifications. This investigation highlighted the paramount importance of vehicle structure deformation behavior in determining overall crashworthiness performance, as the controlled deformation and energy absorption characteristics of the composite airframe directly influenced the acceleration environment experienced by occupants during impact events for integrated seat designs.

Comparisons of the computational ATD model responses with results from full-scale impact tests conducted on a composite fuselage with an integrated seat demonstrated that the simulation could successfully capture the primary impact physics and loading sequences across all body regions. Pelvis acceleration and lumbar loads were validated showing excellent correlation between the model and test since these are the primary metrics for determining the load transferred into the occupant from the impact. Lumbar loads showed a maximum difference of 9% in peak magnitude while the pelvis acceleration showed maximum difference of 13% with excellent match for phase and timing. Thus, they were used to evaluate the effectiveness of various design changes for the integrated composite seats. The chest and head showed similar trends between the test and simulation with some notable differences. The chest prediction of phase and timing was relatively close; however, the magnitude error increased relative to the pelvis at 31% difference. The head showed fair agreement with timing differences attributable to seatback geometry uncertainties. The addition of the seat cushion foam layer was critical to achieving acceptable correlation and enabling proper energy dissipation throughout the impact event. The remaining discrepancies are primarily attributed to: (1) seatback/headrest positioning not exactly matching the test configuration, affecting head response timing; and (2) insufficient seatback compliance modeling, contributing to chest over-prediction. These findings provide confidence in the simulation model's ability to predict occupant loading trends and support design trade studies, while also identifying specific areas for refinement (seatback geometry verification and compliance modeling) if higher fidelity injury prediction is required for future studies. The overall validation quality is suitable for preliminary design analysis, parametric optimization studies, and relative comparisons between design configurations.

The seat leg design was one of the primary focus areas for this study. A single linear leg in the front section was used for the initial design to understand the complex interaction between the seat deformation and the fuselage deformation. In addition, foam materials were also included on the seat that showed limited reduction of loads into the occupant. This study was followed by integrating unique geometry into the seat leg to reduce pelvis acceleration and lumbar loads into the occupant. To this effect, a corrugated seat leg was used. This provided an additional means for reducing the occupant loads and accelerations and minimizing loads below the injury threshold. Another unique design approach that was considered was the frangible seat which allows the seat to separate from the fuselage structure for additional load mitigation. This provided a limited reduction of the impact loads which did manage to reduce the loads below the injury threshold when paired with seat foam and corrugated seat leg. There are several other factors that must be considered for a holistic approach in terms of crashworthiness that were not explored in this study. Some aspects such as maintaining the occupant volume in relation to the flight instrumentation and controls and ensuring a safe path to exit the vehicle can be included for future detailed studies with specific vehicle designs.

This study revealed that implementing energy-absorbing geometric features within the seat attachment structure improved occupant response metrics by providing additional energy dissipation pathways and load distribution mechanisms. These energy-absorbing elements effectively reduced peak accelerations transmitted to the occupant while maintaining structural integrity of the integrated seat system. The parametric design studies conducted using the material model demonstrated that incorporation of crushable zones, optimized attachment geometries, and controlled failure mechanisms within the seat-to-fuselage interface could enhance occupant protection during crash scenarios. These findings provide insights into the design of next-generation electric vertical takeoff and landing vehicles, establishing a foundation for developing composite airframe structures that prioritize both structural efficiency and occupant safety through integrated crashworthiness design principles. The reverse engineering approach developed in this research offers a viable pathway for analyzing existing composite structures and exploring alternative designs for enhanced crash protection performance.

Acknowledgements

The authors would like to acknowledge the use of ChatGSFC Claude 4.5 Sonnet for assisting with editing text for improving clarity and readability.

Reference

[1] Air-. (2018). *Advisory Circular Subject: Methodology for Dynamic Seat Certification by Analysis for Use in Parts 23, 25, 27, and 29 Airplanes and Rotorcraft*.

[2] *TSO-C127c Technical Standard Order Subject: ROTORCRAFT, TRANSPORT AIRPLANE, AND SMALL AIRPLANE SEATING SYSTEMS*. (2020).

[3] *Performance Standard for Seats in Civil Rotorcraft, Transport Aircraft, and General Aviation Aircraft*. (2025). https://doi.org/10.4271/AS8049E

[4] *ARP5765: Analytical Methods for Aircraft Seat Design and Evaluation*. (2012). https://doi.org/10.4271/ARP5765

[5] Littell, Justin. "*The NASA-Langley Gantry: A Visual History of Aircraft and Spacecraft Full-Scale Testing*." Goddard Space Flight Center Engineering Colloquium. 2023.

[6] LSTC. “LS-DYNA Theory Manual”. Livermore Software Technology Company, Livermore, CA. July 2017

[7] Littell, Justin, Jacob Putnam, and Robin Hardy. *The evaluation of composite energy absorbers for use in UAM eVTOL vehicle impact attenuation*. No. NF1676L-31347. 2019.

[8] Fasanella, E. L., & Jackson, K. E. (2004). *Impact Testing and Simulation of a Crashworthy Composite Fuselage Section with Energy-Absorbing Seats and Dummies*. Journal of the American Helicopter Society, *49*(2), 140–148. https://doi.org/10.4050/JAHS.49.140

[9] Hansen, C., & Tsai, T. (1994). Load-limiting landing gear footpad energy absorption system. *NASA. Lewis Research Center, The 28th Aerospace Mechanisms Symposium*.

[10] Jackson, K.E., Fasanella, E.L., and Littell, J.D. “*Development of a Continuum Damage Mechanics Material Model of a Graphite-Kevlar ® Hybrid Fabric for Simulation the Impact Response of Energy Absorbing Subfloor Concepts*.” Proceedings from the 73rd Annual American Helicopter Society Annual Forum and Technology Display. Fort Worth, TX. May 9-11, 2017

[11] S. Guha, "*LSTC_NCAC Hybrid III 50th Dummy Positioning & Post-Processing*," ed. LSTC Michigan, 2014.

[12] *Instrumentation for Impact Test, Part 1 - Electronic Instrumentation SAE J211. (2022).* https://doi.org/10.4271/J211/1_202208

[13] *eCFR :: 14 CFR 27.562 -- Emergency landing dynamic conditions. (FAR 27.562)*. (n.d.). Retrieved March 18, 2026, from https://www.ecfr.gov/current/title-14/chapter-I/subchapter-C/part-27/subpart-C/subject-group-ECFRf2515baf1391800/section-27.562

[14] *eCFR :: 14 CFR 25.562 -- Emergency landing dynamic conditions. (FAR 25.562)*. (n.d.). Retrieved March 18, 2026, from https://www.ecfr.gov/current/title-14/chapter-I/subchapter-C/part-25/subpart-C/subject-group-ECFRda24a9b1d389632/section-25.562

[15] Putnam, Jacob, and Justin Littell. "*Simulation and analysis of NASA lift plus cruise evtol crash test*." Vertical Flight Society's 79th Annual Forum. 2023.

[16] Littell, Justin D., Jacob B. Putnam, and Nathaniel W. Gardner. *A Summary of Structural Test and Simulation Results for Hawker 4000 Composite Fuselage Hardware*. No. NASA/TM-20230012644. National Aeronautics and Space Administration, 2023.

[17] Putnam, Jacob B. *Occupant Response Analysis of a Full-Scale Crash Test of a Fokker F28 Fellowship Aircraft*. No. NF1676L-35990. 2020.

[18] DeWeese, Richard L., David M. Moorcroft, and Amanda M. Taylor. "*Lumbar load variability in dynamic testing of transport category aircraft seat cushions*." (2021).

[19] Johnson, W., Silva, C., and Solis, E. "*Concept Vehicles for VTOL Air Taxi Operations.*" Proceedings from the AHS Technical Conference on Aeromechanics Design for Transformative Vehicle Flight. San Francisco, CA. January 16- 19, 2018.

[20] Putnam, Jacob, and Justin Littell. "*Evaluation of impact energy attenuators and composite material designs of a UAM VTOL concept vehicle*." VFS Annual Forum and Technology Display. No. NF1676L-31376. 2019.